

Molecular Dynamics Studies on Glass Formation of Pd-Ni Alloys by Rapid Quenching

S. ÖZDEMİR KART¹, M. TOMAK², M. ULUDOĞAN³, T. ÇAĞIN³

¹*Department of Physics, Pamukkale University, Kınıklı Campus, 20020, Denizli-TURKEY*

²*Department of Physics, Middle East Technical University, 06531 Ankara-TURKEY*

³*Department of Chemical Engineering, Texas A&M University, Texas, TX 77845-3122, USA*

Received 18.07.2006

Abstract

The rapid solidification of Pd-Ni alloys is studied with the constant-pressure and constant-temperature (TPN) and the constant-volume and constant-temperature (TVN) molecular dynamics technique to obtain an atomic description of glass formation in the alloy. Quantum Sutton-Chen potential for Pd-Ni binary system is applied in the simulations. We present some thermodynamic and structural results from simulations of such glasses over a range of compositions. The structural properties are analyzed by means of pair distribution function, volume, and enthalpy as a function of temperature and concentration at the cooling rates ranging from 5 K/ps to 0.05 K/ps to see whether the Pd-Ni alloy goes into glass formation or it crystallizes. The relation between the cooling rate and glass transition temperature is revealed. We have also investigated shear viscosity in the supercooled regime. Its temperature dependence indicates fragile-liquid behavior, typical of binary metallic glasses. The results shows that the atomic mismatch and having the eutectic composition are important parameters to form glassy state.

Key Words: Molecular dynamics, metallic glass, glass transition, fragility and Wendt-Abraham parameter.

1. Introduction

When liquid metal is cooled down, either crystalline solid or amorphous solid is obtained depending on the cooling rate. If the cooling rate is sufficiently high, homogeneous nucleation of crystalline phases can be completely avoided, and thus the metastable amorphous structure is formed. Metallic glasses have been widely used due to their unusual magnetic and mechanical properties, as well as wear and corrosion resistance [1].

Metallic glasses have generated considerable scientific interest since the first discovery of amorphous metallic alloy by Duwez et. al. [2]. The conventional (mostly binary) metallic glass forming alloys must be rapidly quenched with rates up to 10^6 K/s for vitrification. The thickness of such samples is limited to the μm regime, but preventing the practical applications of the amorphization technique. More recently, bulk metallic glasses (BMG) have been developed with much lower critical cooling rates of 100 K/s to 1 K/s [3, 4]. These much lower cooling rates give rise to a much higher critical thickness of up to several cm, making it possible to perform experimental investigations of the glass transition and the undercooled liquid state of a metallic system.

Johnson has constructed an effective way of designing BMG with high glass forming ability [4]: His strategy consists of choosing the binary alloys with deep eutectic composition, and then adding suitable components to obey three empirical rules developed by Inoue [5] for the achievement of high glass forming ability in metallic glasses formed. Having at least three elements, the mismatch in the atomic size and having

negative heats of mixing among the constituent elements serve as a guiding principle for the selection of elements. However, the issue of glass-forming ability of the metals is not yet fully understood. Therefore the knowledge of the structural, thermodynamic and atomic-transport properties is essential for the explanation of such a phenomenon.

The acceptable formation mechanism of amorphous metal glasses is not available. Molecular dynamics (MD) simulation can provide the opportunity to understand the nature of the glass formation at an atomic level, which is difficult to access in real experiments or hard to obtain with reasonable precision. There are large number of studies in the MD simulations of glass transitions of metals and binary alloys [6–23].

Pd-Ni metallic alloy has a eutectic region around 45 % of Pd [24]. Pd and Ni have very different sizes, making them good candidates for forming a metallic glass. Our interest in this material is also related to its ability to form a basis for development of some industrially important BMG, such as Pd-Ni-P [25, 26], and Pd-Ni-Cu-P [27, 28]. Hence, we are interested in the properties of undercooled Pd-Ni alloys by performing MD simulations using quantum Sutton-Chen potentials [29] whose performance on solid and liquid pure Pd and Ni metals and their binary alloys has been investigated in our previous studies [30, 31]. The Pd-Ni alloys are quenched at different cooling rates to see whether the system goes into glass formation or it crystallizes.

2. Interatomic Potential and Computational Procedure

The molecular dynamics simulation performed in this study uses the Sutton-Chen (SC) type potential [32]. This potential is recently parameterized by Çağın et al. [29] by including quantum corrections accounting for zero-point energy, hence called quantum Sutton-Chen (Q-SC) potential, to improve some physical properties at high temperatures. The potential parameters are obtained by fitting to some experimental properties, such as lattice parameter, cohesive energy, bulk modulus, phonon frequency at the X point, vacancy formation energy and surface energy.

The SC interaction potential comprises a pair potential $V(r_{ij})$ between atoms i and j , responsible for the Pauli repulsion between the core electrons and a local energy density ρ_i term accounting for cohesive interaction associated with atom i . The total potential energy has the following form:

$$U_{tot} = \sum_i U_i = \sum_i \left[\sum_{j \neq i} \frac{1}{2} \epsilon_{ij} V(r_{ij}) - c_i \epsilon_{ij} (\rho_i)^{\frac{1}{2}} \right], \quad (1)$$

where,

$$V(r_{ij}) = \left(\frac{a_{ij}}{r_{ij}} \right)^{n_{ij}}, \quad (2)$$

and

$$\rho_i = \sum_{j \neq i} \phi(r_{ij}) = \sum_{j \neq i} \left(\frac{a_{ij}}{r_{ij}} \right)^{m_{ij}}. \quad (3)$$

In the Eqs. 1-3, r_{ij} is the distance between atoms i and j , a is a length parameter leading to dimensionless for $V(r_{ij})$ and ρ_i , c is a dimensionless parameter scaling the attractive term relative to the repulsive term, ϵ sets the overall energy scale, and n , m are positive integer parameters such that $n > m$.

We adopt the random binary fcc metal alloy method developed by Rafii-Tabar and Sutton [33]; two types of atoms occupy the sites randomly such that the alloy has the required average concentration, to produce the potential parameters for Pd-Ni alloys. The following combination rules are utilized in describing the interaction between different types of atoms;

$$\epsilon_{ij} = \sqrt{\epsilon_i \epsilon_j}, \quad (4)$$

$$a_{ij} = \frac{a_i + a_j}{2}, \quad (5)$$

$$m_{ij} = \frac{m_i + m_j}{2}, \quad (6)$$

$$n_{ij} = \frac{n_i + n_j}{2}. \quad (7)$$

The values of the Q-SC potential parameters for Pd and Ni are given in Table 1.

Table 1. Quantum Sutton-Chen (Q-SC) [29] potential parameters for Pd and Ni.

metal	n	m	ϵ (meV)	c	a (Å $^\circ$)
Pd	12	6	3.2864	148.205	3.8813
Ni	10	5	7.3767	84.745	3.5157

The system composed of 864 atoms is firstly heated from 0.1 K to 2000 K by using the algorithm based on extended Hamiltonian formalism [34–38]. The details of heating procedure is presented in our previous study [30]. The system is run for 50000 time steps at 2000 K to guarantee an equilibrium liquid state to obtain the initial configuration for the cooling process, which are carried out by using isothermal-isobaric (TPN) and canonical (TVN) MD dynamics. The alloy is then cooled to 100 K with decrements of 100 K at four different cooling rates of 5 K/ps, 1 K/ps, 0.5 K/ps, and 0.05 K/ps, corresponding to MD steps of 10^4 , 5×10^4 , 10^5 , and 10^6 , respectively. The simulation time step is chosen as 0.002 ps. Some macroscopic description of the system, such as volume, energy and structure are obtained from the TPN MD cooling runs. The densities obtained from TPN cooling runs for each cooling rate are utilized as input parameters to perform TVN simulations. About 5 % of time steps for TVN MD dynamics are carried out for equilibrium of the system for each cooling rate to consider the effects of the sudden volume changes. Finally, production runs are performed to obtain some transport properties, such as shear viscosity.

3. Results

The enthalpy of $\text{Pd}_{0.45}\text{Ni}_{0.55}$ as a functions of temperature is given in Figure 1 during heating and cooling process at four kinds of cooling rates. The large jump in the enthalpy in the temperature of range of 1500 K to 1600 K for heating process is due to the melting of the Pd-Ni alloy. The enthalpy drops linearly with decreasing temperature and there is little difference in the enthalpy changes between the different cooling rates in the high-temperature region between 2000 K and melting point. In the low temperature region, when the temperature is below about 1100 K, the enthalpy changes shows a big difference between the different cooling rates. When the slower cooling rate of 0.05 K/ps is used in the simulation, the enthalpy is observed to have big break with decreasing temperature, which shows that liquid to crystallization transition occurs. At this cooling rate, the atoms in liquid have enough time to move its particular neighbor positions and crystal occurs. By contrast, when we adopt faster cooling rates between 5 K/ps to 0.5 K/ps to simulate the cooling process, there is no sharp drop of enthalpy, only the slope of enthalpy curves becomes lower in the low temperature region. The discontinuity in slope indicates a liquid to amorphous transition or a glass transition. Under these cooling conditions, the atoms in liquid move more and more slowly as a supercooled liquid is cooled to lower temperatures because the viscosity of the liquid increases continuously. Finally, atomic motion is frozen on the time scale of the cooling process and a glass forms.

We examine the structural features of $\text{Pd}_{0.45}\text{Ni}_{0.55}$ in the liquid, supercooled liquid, amorphous and crystal states in Figure 2 by analyzing the pair distribution function, $g(r)$, during heating process and cooling process at two different quenching rates. The system with a random fcc crystal is heated to 2000 K and cooled back to 1900 K (above T_m). At 1900 K, the system is in a liquid state, both in heating and cooling processes as shown in Figure 2a. At the temperature of 1300 K (Figure 2b) in the cooling process, although the temperature is lower than the melting point of $\text{Pd}_{0.45}\text{Ni}_{0.55}$, the system is still in a liquid (super-cooled) state. Cooling to 300 K at the fast quenching rate of 5 K/ps, see Figure 2c, the second peak of $g(r)$ splits into two subpeaks, which indicates the formation of metallic glass. On the other hand, when cooling down to 700 K at the slow quenching rate of 0.05 K/ps, see Figure 2d, the first peak becomes very high and many small peaks appear, which shows that the system goes into crystalline state.

We have also obtained the glass transition temperature T_g by using the Wendt-Abraham parameter [39], defined by $R = g_{min}/g_{max}$, where g_{max} and g_{min} are the magnitudes of the first shell maximum and the first minimum following the maximum in the pair distribution function, respectively. Figure 5 gives the Wendth-Abraham parameters for the eutectic region quenching at three different rates as the temperature

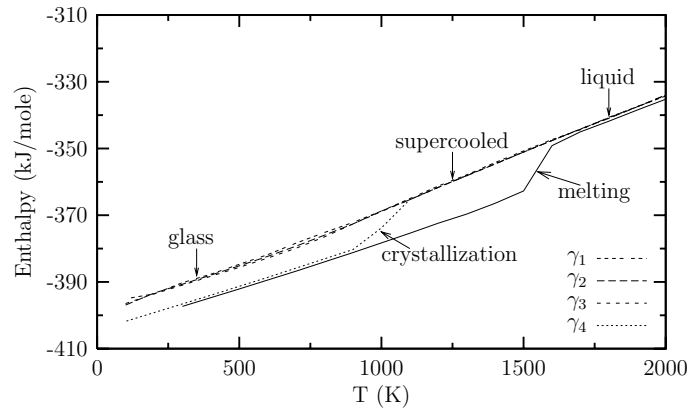


Figure 1. The enthalpy of $\text{Pd}_{0.45}\text{Ni}_{0.55}$ versus the temperature during the heating and cooling processes at the cooling rates of $\gamma_1 = 5 \text{ K/ps}$, $\gamma_2 = 1 \text{ K/ps}$, $\gamma_3 = 0.5 \text{ K/ps}$, $\gamma_4 = 0.05 \text{ K/ps}$

varies. As shown in the figure, there exist two lines with different slopes and their intersections are the glass transition temperatures T_g , which are 710 K, 670 K, and 660 K for the cooling rates of 5 K/ps, 1 K/ps, and 0.5 K/ps, respectively. Thus, the glass transition temperature increases with increased cooling rate. The fastest cooling rates result in shorter times for the atoms to relax thus leading to formation of the glass at a higher temperature than at lower cooling rate.

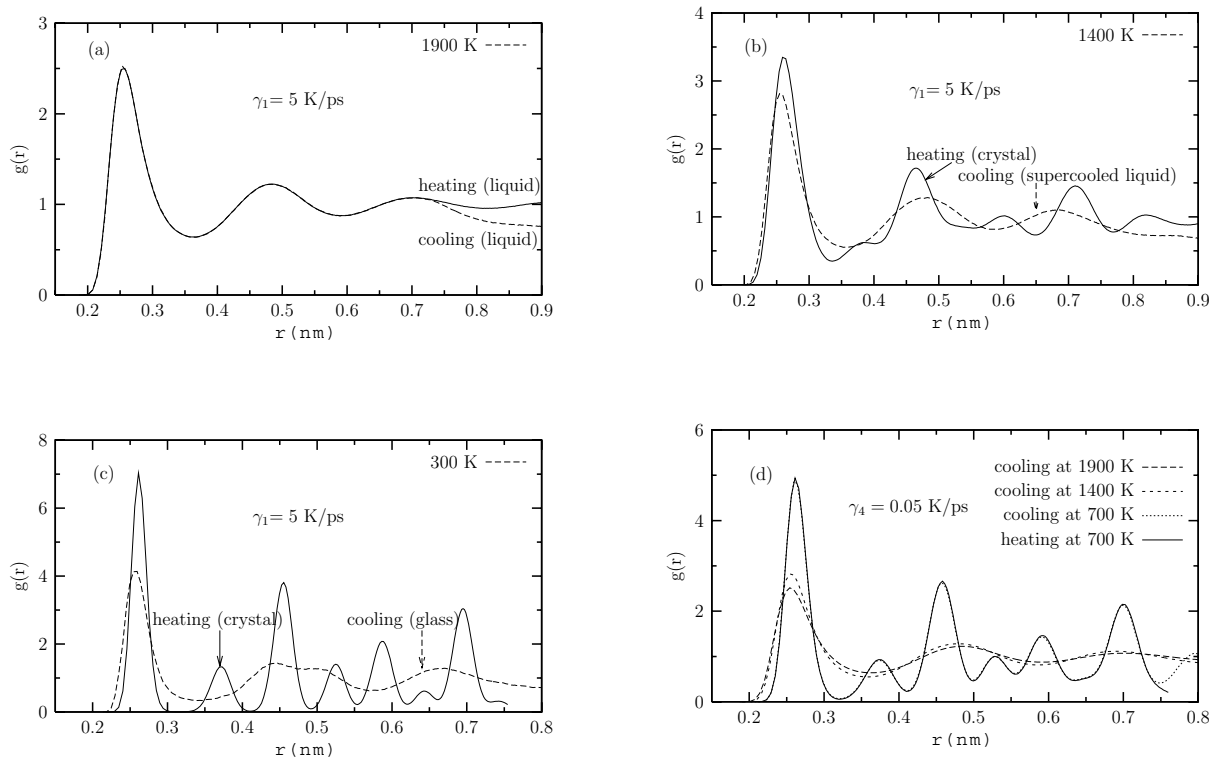


Figure 2. Pair distribution function $g(r)$ of $\text{Pd}_{0.45}\text{Ni}_{0.55}$ during the heating (solid lines) and cooling (dashed lines) processes a) at 1900 K (liquid state), b) at 1400 K (supercooled liquid), c) at 300 K (amorphous state) at the fast cooling rate of $\gamma_1 = 5 \text{ K/ps}$, and c) at 1900 K (liquid state), 1400 K (supercooled liquid), and 700 K (crystalline state) at the slow cooling rate of $\gamma_4 = 0.05 \text{ K/ps}$.

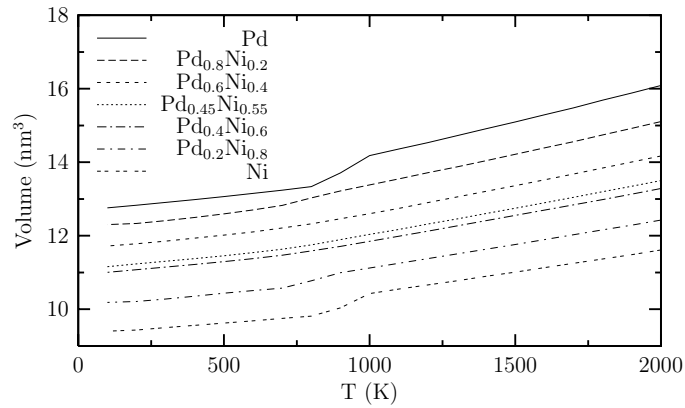


Figure 3. The volume of Pd-Ni alloys as a function of temperature during cooling process at the rate of $\gamma_3 = 0.5$ K/ps

The concentration effects on the glass transition are analyzed by depicting volume of Pd-Ni alloys as a function of concentration. This graph is given in Figure 3. As seen from the figure, the glass transitions are observed as approaching towards the eutectic region, while pure Pd and Ni and concentration at 20 % of Pd form ordered state at the cooling rate of 0.5 K/ps. For the concentration of $\text{Pd}_{0.8}\text{Ni}_{0.2}$, it can be seen that the volume curve is different from both those volume curves showing crystallization and those volume curves showing glass formation. This is further confirmed by $g(r)$ at room temperature in Figure 4. The left subpeak is significantly higher than the right subpeak observed in the second peak of $g(r)$, which shows that the final phase is a partially crystallized amorphous structure, while $g(r)$ of $\text{Pd}_{0.6}\text{Ni}_{0.4}$ show a typical amorphous structure.

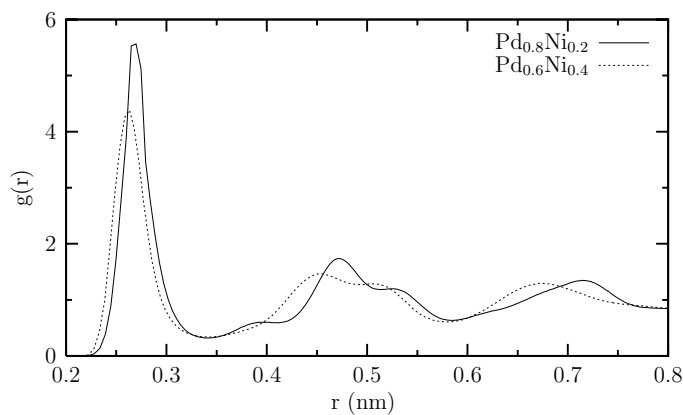


Figure 4. Pair distribution function $g(r)$ of $\text{Pd}_{0.8}\text{Ni}_{0.2}$ and $\text{Pd}_{0.6}\text{Ni}_{0.4}$ at room temperature at the cooling rate of $\gamma_3 = 0.5$ K/ps.

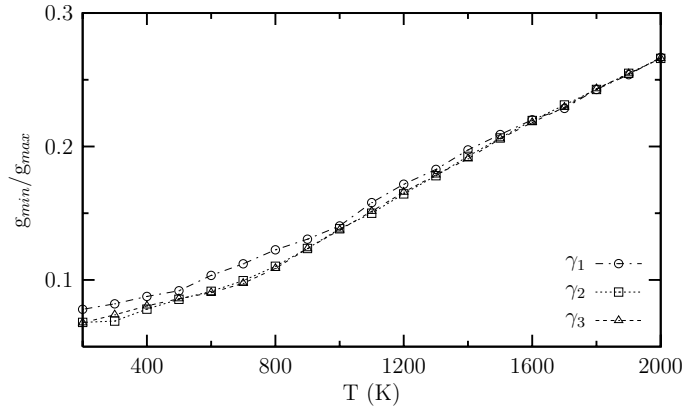


Figure 5. Wendt-Abraham parameter (g_{min}/g_{max}) versus temperature for eutectic composition obtained from three different cooling rates ($\gamma_1=5$ K/ps, $\gamma_2=1$ K/ps, and $\gamma_3=0.5$ K/ps).

The T_g of Pd-Ni are also computed to study the concentration effects on T_g . Table 2 gives the values of T_g obtained by Wendt-Abraham parameter from intercept method for Pd-Ni alloys at the cooling rates of 5 K/ps and 0.5 K/ps. When the system is quenched at the rate of 5 K/ps, glass transition temperatures of pure Pd, and Ni are nearly the same, while those of Pd-Ni alloys increase with increasing fraction of Pd, due to the increase in the viscosity in the alloy case. Greater viscosity results in less time for atoms to relax, thus reflecting the glass formation at a higher temperature. As far as the cooling rate of 0.5 K/ps is concerned, the system at the eutectic and near-eutectic regions goes into glass formation while the substance forms crystalline state at the non-eutectic composition. This shows that the mismatch in atomic size and having the eutectic composition are favorable to glass formation.

Table 2. Glass transition temperatures (T_g) for Pd-Ni alloys at two different cooling rates.

Metal	T_g (K)	
	$\gamma_2=5$ K/ps	$\gamma_4=0.5$ K/ps
Ni	810 ± 13	crystal
$Pd_{0.2}Ni_{0.8}$	645 ± 3	crystal
$Pd_{0.4}Ni_{0.6}$	690 ± 31	630 ± 23
$Pd_{0.45}Ni_{0.55}$	710 ± 30	660 ± 20
$Pd_{0.6}Ni_{0.4}$	710 ± 14	690 ± 26
$Pd_{0.8}Ni_{0.2}$	738 ± 1	crystal-glass
Pd	799 ± 3	crystal

We are also interested in understanding the dynamics of the supercooled liquid regions by studying the transport property like viscosity in this work. The departure from the Arrhenius law in the viscosity is the most important characteristic feature of the glass forming liquids. The fragility concept measures the degree with which the viscosity of a supercooled liquid deviates from the Arrhenius behavior. Hence we are particularly interested in the viscosity of eutectic region at the cooling rate of 0.5 K/ps. The shear viscosity η is calculated from the Green-Kubo (GK) relation [40] by performing MD simulations at TVN dynamics. Figure 6 shows Arrhenius plot of the equilibrium viscosity data of the $Pd_{0.45}Ni_{0.55}$ supercooled liquids in which the temperatures are normalized by the glass-transition temperature T_g . Use of glass transition temperature T_g as the scaling temperature for viscosity allows for classification of liquid according to their strong-fragile behavior. Strong liquids show close to Arrhenius temperature dependence of viscosity and form glasses. Fragile liquids, on the other hand, show low viscosity at the melting temperature only to rise sharply close to the glass transition and form glasses which are unstable with respect to crystallization. In order to quantify the fragility, Angell and co-workers[41, 42] introduced a fragility parameter m , defined as;

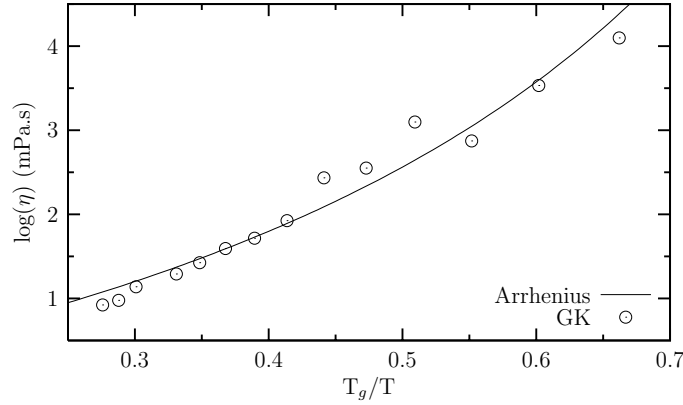


Figure 6. Temperature dependence of shear viscosity coefficient η for eutectic composition at the rate of $\gamma_3=0.5$ K/ps. Circles: Simulation results obtained from Green-Kubo (GK) relation. Solid line: Arrhenius fit.

$$m = \left. \frac{d \log \eta}{d(T_g/T)} \right|_{T=T_g} \quad (8)$$

The Eq. 8 presents a measure of the steepness of the slope of the viscosity curve at T_g when the temperature is scaled by T_g ; that is, a larger value of m means a greater deviation from Arrhenius behaviors. The fragility parameter m is about 20 for strong liquid extreme and about 200 for fragile liquid extreme [41, 42]. We find the fragility index as 112 for $\text{Pd}_{0.45}\text{Ni}_{0.55}$ at the cooling rate of 0.5 K/ps, reflecting that eutectic liquid is classified into fragile liquid. The result is in good agreement with the values of the fragility parameter ranging $86 \leq m \leq 121$ investigated by Komatsu [43] for metallic alloys consisting of binary and ternary systems. The fragility is quantified alternatively by the strength parameter D^* in the Vogel-Fulcher Tamman (VFT) relation;

$$\eta(T) = \eta_0 \exp(D^* T_0 / (T - T_0)) \quad (9)$$

where η_0 and D^* are fitting parameters, and T_0 is the VFT temperature that is usually below T_g . The values of the strength parameter are around 100 for strong liquids and less than 10 for fragile liquids [41, 42]. Our data for eutectic region and near-eutectic region are fitted to the VFT equation. D^* of $\text{Pd}_{0.4}\text{Ni}_{0.6}$, $\text{Pd}_{0.45}\text{Ni}_{0.55}$, $\text{Pd}_{0.6}\text{Ni}_{0.4}$ evaluated at the cooling rate of 0.5 K/ps are, 3.79, 5.76, and 4.53, respectively. Therefore, the eutectic composition has the highest value of D^* , reflecting that the liquid having eutectic composition has the highest glass forming ability. We get low strength parameters, which shows that Pd-Ni system is a fragile liquid.

4. Conclusion

In this paper, a series of simulations is performed to investigate the phase transformation of Pd-Ni alloys during heating and rapid cooling processes. It is found that eutectic region forms an fcc crystal structure at the slow cooling rate of 0.05 K/ps, while amorphous structure is obtained at the rates of 5 K/ps, 1 K/ps and 0.5 K/ps. The mismatch in atomic size and having the eutectic composition play an important role in glass formation, leading to glass formation of eutectic and near-eutectic compositions and crystalline formation of Pd, Ni, and $\text{Pd}_{0.2}\text{Ni}_{0.8}$ at the intermediate cooling rate of 0.5 K/ps. The glass transition temperature depends on the quenching rate; the larger the quenching rate, the higher the glass transition temperature. The fragility parameter is calculated from viscosity data fitted to Arrhenius relation. Viscosity data above glass transition temperature indicate that Pd-Ni binary metal alloys are the fragile glass former according to Angell's classification [41, 42]. The results for the strength parameter obtained from VFT relations show that the eutectic composition has the highest glass forming ability.

Acknowledgments

This work is financially supported by TUBITAK Project No: TBAG-HD/49(105T261) and Middle East Technical University Research Fund through Project No: BAP-2002-01-05-07.

References

- [1] C. Fan, A. Takeuchi, and A. Inoue, *Mater. Trans. JIM*, **40**, (1999), 42.
- [2] P. Duwez, R. H. Willens, and W. Klement, *J. Appl. Phys.*, **31**, (1960), 1137.
- [3] A. Peker and W. L. Johnson, *Appl. Phys. Lett.*, **63**, (1993), 2342.
- [4] W. L. Johnson, *MRS Bull.*, **24**, (1999), 42.
- [5] A. Inoue, *Bulk Amorphous Alloys: Preparation and Fundamental Characteristics, Material Science Foundations*, Vol. 4, (Trans. Tech., Amsterdam, 1998).
- [6] K. Chen, H. Liu, X. Li, Q. Han, Z. Hu, *J. Phys.: Condens. Matter*, **7**, (1995), 2379.
- [7] C. S. Liu, Z. G. Zhu, J. Xia, and D. Y. Sun, *J. Phys.: Condens. Matter*, **13**, (2001), 1873.
- [8] G. X. Li, Y. F. Liang, Z. G. Zhu, and C. S. Liu *J. Phys.: Condens. Matter*, **15**, (2003), 2259.
- [9] C. S. Liu, J. Xio, Z. G. Zhu, and D. Y. Sun, *J. Chem. Phys.*, **114**, (2001), 7506.
- [10] L. Wang, H. Liu, K. Chen and Z. Hu, *Physica B*, **239**, (1997), 267.
- [11] K. Vollmayr, W. Kob, and K. Binder, *J. Chem. Phys.*, **105**, (1996), 4714.
- [12] E. G. Noya, C. Rey, and L. J. Gallego, *J. Non-Cryst. Solids*, **298**, (2002), 60.
- [13] L. Wang, X. Bian, and J. Zhang, *J. Phys. B: At. Mol. Opt. Phys.*, **35**, (2002), 3575.
- [14] Y. Qi, T. Çağın, Y. Kimura, and W. A. Goddard III, *Phys. Rev. B*, **59**, (1999), 3527.
- [15] L. Qi, H. F. Zhang, and Z. Q. Hu, *Intermetallics*, **12**, (2004), 1191.
- [16] H. H. Kart, M. Uludoğan, T. Çağın, and M. Tomak, *J. Non-Cryst. Solids*, **342**, (2004), 6.
- [17] T. Aihara, K. Aoki, and T. Masumoto *Mater. Sci. Eng. A* **179** (1994) 256; T. Aihara, Y. Kawazoe, and T. Masumoto, *J. Non-Cryst. Solids*, **207**, (1996), 875.
- [18] H. Teichler, *Phys. Rev. E*, **53**, (1996), 4287.
- [19] F. Delogu, *Mater. Sci. Eng. A*, **359**, (2003), 52.
- [20] M. Shimono, and H. Onodera, *Mater. Trans. JIM*, **39**, (1998), 147.
- [21] Q. X. Pei, C. Lu, and M. W. Fu, *J. Phys.: Condens. Matter*, **16**, (2004), 4203.
- [22] N. P. Bailey, J. Schiøtz, and K. W. Jacobsen, *Phys. Rev. B*, **69**, (2004), 144205.
- [23] L. Qi, H. F. Zhang, Z. Q. Hu, and P. K. Liaw, *Physics Letters A*, **327**, (2004), 506.
- [24] R. Hultgren, D. D. Desai, and D. T. Hawkins, *Selected Values of Thermodynamic Properties of Binary Alloys*, (ASM, Metals Park OH, 1973).
- [25] Z. P. Lu, Y. Li, and S. C. Ng, *J. Non-Cryst. Solids*, **270**, (2000), 103.
- [26] A. Inoue and N. Nishiyama, *Mater. Sci. Eng. A*, **226-228**, (1997), 401.
- [27] N. Nishiyama and A. Inoue, *Mater. Trans. JIM*, **37**, (1996), 1531.
- [28] J. Schroers and W. L. Johnson, *Appl. Phys. Lett.*, **80**, (2002), 2069.

- [29] T. Çağın, Y. Qi, H. Li, Y. Kimura, H. Ikeda, W. L. Johnson, and W. A. Goddard III, *MRS Symp. Ser.*, **554**, (1999), 43.
- [30] S. Özdemir Kart, M. Tomak, M. Uludoğan, and T. Çağın, *J. Non-Cryst. Solids*, **337**, (2004), 101.
- [31] S. Özdemir Kart, M. Tomak, and T. Çağın, *Physica B*, **355**, (2005), 382.
- [32] A. P. Sutton and J. Chen, *Phil. Mag. Lett.*, **61**, (1990), 139.
- [33] H. Rafii-Tabar and A. P. Sutton, *Phil. Mag. Lett.*, **63**, (1991), 217.
- [34] H. C. Andersen, *J. Chem. Phys.*, **72**, (1980), 2384.
- [35] M. Parrinello and A. Rahman, *Phys. Rev. Lett.*, **45**, (1980), 1196.
- [36] S. Nosé, *J. Chem. Phys.*, **81**, (1984), 511.
- [37] W. G. Hoover, *Phys. Rev. A*, **31**, (1985), 1695.
- [38] T. Çağın and B. M. Pettitt, *Mol. Phys.*, **72**, (1991), 169; T. Çağın and B. M. Pettitt, *Mol. Sim.*, **6**, (1991), 5.
- [39] H. R. Wendt and F. F. Abraham, *Phys. Rev. Lett.*, **41**, (1978), 1244.
- [40] M. P. Allen and D. J. Tildesley, *Computer Simulation of Liquids*, (Oxford Science Publications, New-York, 1987).
- [41] C. A. Angell, *Science*, **267**, (1995), 1924; C. A. Angell, *J. Non-Cryst. Solids*, **131-133**, (1991), 13; C. A. Angell, B. E. Richards and V. Velikov, *J. Phys: Condens. Matter*, **11**, (1999), A75.
- [42] R. Böhmer, K. L. Ngai, C. A. Angell, D. J. Plazek, *J. Chem. Phys.*, **99**, (1993), 4201.
- [43] T. Komatsu, *J. Non-Cryst. Solids*, **185**, (1995), 199.